ACS APPLIED NANO MATERIALS



Article

# Polymer nanocomposite-based strain sensors with tailored processability and improved device integration

Pedro Costa, M. Fátima Carvalho, Vitor Correia, Julio C Viana, and Senentxu Lanceros-Méndez

*ACS Appl. Nano Mater.*, **Just Accepted Manuscript** • DOI: 10.1021/acsanm.8b00647 • Publication Date (Web): 24 May 2018



ACS Publications

is published by the American Chemical Society. 1155 Sixteenth Street N.W., Washington, DC 20036

# Polymer Nanocomposite-Based Strain Sensors with Tailored Processability and Improved Device Integration

Pedro Costa[1,2*], Maria Fátima Carvalho[1], Vitor Correia[1,3], Júlio César Viana[2], Senentxu Lanceros-Mendez[4,5]

1- Center of Physics, University of Minho, 4710-058 Braga, Portugal
2- Institute for Polymers and Composites (IPC), University of Minho, 4800-058 Guimarães, Portugal
3- Algoritmi Research Center, University of Minho, Guimarães, Portugal
4- BCMaterials, Basque Center for Materials, Applications and Nanostructures, UPV/EHU Science Park, 48940 Leioa, Spain
5- IKERBASQUE, Basque Foundation for Science, 48013 Bilbao, Spain
*Corresponding author: pcosta@fisica.uminho.pt

## Abstract

Due to its easy processability and elastomeric properties, the triblock copolymer styrene-butadiene-styrene (SBS) is an excellent matrix for the development of piezoresistive polymer composites, mostly for larger strain composites. Piezoresistive sensors based in SBS and conductive fillers have been processed by scalable methods, extrusion and spray printing, allowing the measurement of large deformations up to 20% of strain with low mechanical hysteresis in loading-unloading cycles. The carbon nanotube (CNT) reinforcement increases the mechanical properties (maximum stress and strain) and provides electrical properties to the composites. Extruded and spray printed carbon nanotubes (CNT)/SBS composites show a piezoresistive sensibility (gauge factor) up to 4 and 2, respectively. Their percolation threshold is near 6 and 1 wt.%, for extruded and spray printed methods, respectively. The excellent piezoresistive reproducibility, processability and easy integration in structures and devices show the suitability of those materials for applications, as demonstrated by the implementation of a hand glove able to measure the movement of the fingers. The electronic readout systems develop allows, in real-time, measure and save the data points of each piezoresistive sensor in a remote platform. Thus, the present paper demonstrates the optimisation, processing by scalable methods, and integration of piezoresistive polymer-based materials for force and deformation sensor applications.

**Keywords:** Polymer composites; Piezoresistive; Stretchable materials; Electronic system; Device application; Thermoplastic Elastomers

## 1. Introduction

The fast development of materials science and nanotechnology allows tailoring materials properties to reach ever more demanding application requirements[1]. Thus, smart and multifunctional materials are of increasing interest from the scientific point of view and in applications as high performance sensors and actuators[2-4], being used for the development of pressure/compression[1, 5-7], deformation[4-6], touch[8], humidity[9] and temperature[4, 10] sensors, among others[11]. Within the different areas of interest, biomedical and structural health monitoring (SHM) evidence a large increase in research and device applications[12-13].

Among the most used sensors are the ones used to monitor mechanical variations related to the application of pressure, deformation or bending[14]. Within the different physical principles and sensors that can be applied, piezoresistive materials and strain gauges are among the most relevant ones due to their low cost, high sensibility and repeatability compared others sensor types[14]. Thus, the piezoresistive response of different materials has been explored for the development of strain sensors, including commercial metal-foil strain gauges[15], crystalline silicon[16], polymer composites or intrinsically conductive polymers[17-18]. In this way, there are a wide range of commercial piezoresistive sensors (mainly metallic strain gauges), which can be used for force[19], pressure[20-21] and inertia[22] measurements. The major limitation of current solutions, which has been addressed in the present work, is that they are difficult to apply for large deformation sensors and also difficult to integrate into devices. Polymer-based piezoresistive materials can provide solution to those aspects and can be fabricated by different processing methods from a wide variety of polymers as matrices, including epoxies[23], thermoplastics[17, 24] and elastomers[6, 14, 25], reinforced by semiconducting and conducting nanofillers[4, 26] of different geometries, being mainly carbonaceous fillers with different aspect ratios[27]. The above mentioned parameters have strong influence in the overall properties of the composites[28] and, in particular, in their piezoresistive response. Polymer composites for strain sensing applications have been prepared with metallic particles[29], carbon black[28], carbon nanofibers[30], carbon nanotubes[31] or combinations of carbon materials[7] as fillers and with different polymer matrices, to tailor the mechanical properties of the composite[32].

Thus, polymer-based composites are excellent candidates for the development of piezoresistive sensors due to their large versatility with respect to their mechanical properties, lightweight, easy processing, low cost and larger piezoresistive response[4, 33-34]. There are several studies in epoxy and thermoplastic polymer composites for sensing applications[35-36], however these polymers shows a stretchability below 5% of strain, being comparable to the one of commercial strain gauges[5, 37]. Stretchability, on the other hand, is one of the main characteristics of elastomeric materials, with large strain and easy recovery, being the most suitable polymer matrixes for large deformation sensors applications[4, 38]. Further, it has been shown that elastomeric composites with carbonaceous nanofillers show no relevant aging under UV and humidity conditions[39] and can be biocompatible[38, 40], for the development of biomedical applications.

These sensors can be produced by a wide range of polymer processing techniques, including printing technologies[41], such as screen printing, spray printing or inkjet printing or industrial techniques such as injection moulding or extrusion[34, 42]. This allow not only low-cost production, but also easy integration into devices or the development of functional structural parts with integrated self-sensing characteristics[33], which is essential for the development of the industry 4.0 concept[43-44] as well as in areas such as aeronautics or robotics[14].

An essential part of the development of piezoresistive sensors solutions consists in the corresponding electronic readout system[45]. The fast development of micro- and nanotechnologies enabled the miniaturization of sensors and the physical integration of various functions and signal processing elements in the same substrate, allowing better integration. Thus, the integrated system can provide real time monitoring[46] with high levels of reliability in the parameters being measured and wireless communicated[47].

The piezoresistivity or sensibility under strain is quantitatively expressed as the gauge factor ($GF$[48]) and is defined as the ratio between the relative electric resistance variation and the mechanical strain applied to the material ($\varepsilon = {}^{\Delta l}/_{l_0}$), as expressed in equation 1:

$$GF = \frac{{}^{\Delta R}/_{R_0}}{\varepsilon} = \frac{{}^{\Delta \rho}/_{\rho_0}}{\varepsilon} + 1 + 2\nu \quad (1)$$

where, $R_0$ is the electrical resistance of the sample without mechanical deformation and $\Delta R$ is the resistance change caused by the variation in length ($\Delta l$). $\rho$ is the electrical resistivity and the $\nu$ is the Poisson ratio[34, 49]. Equation 1 shows that the $GF$ has contributions from the geometrical effect (1+2$\nu$) and an intrinsic component ($\frac{\Delta\rho/\rho}{\varepsilon}$)[49]. The Poisson ratio values for polymers typically range from 0.35 to 0.5[50]. With those values of the Poisson ratio, the geometric contribution of the *GF* can range between 1.7 and 2 (equation 1) and therefore, *GF* lower than 2 can be attributed to geometric contributions and values above 2 are attributed to intrinsic electrical resistivity variations with the applied strain in composite. Large number of studies have recently demonstrated that thermoplastic elastomer composites with conducting nanofillers show significant piezoresistive performance with high sensitivity and mechanical deformations above 20%[51]. These composites can be processed by solvent casting[49] or extruded[34], and from commercial to laboratory synthetized[52] allowing new implementation areas, using as stretchable piezoresistive sensors.

In this context, the present work reports on the development of polymer-based piezoresistive composites processable either by extrusion and by spray printing techniques, allowing the scalable production of the sensors as well as improved integration in to devices[53]. The composites are based on carbon nanotubes (CNT) dispersed in a thermoplastic elastomer matrix based of the triblock copolymer styrene-butadiene-styrene (SBS). Polymer-based composites with CNT present low electrical percolation threshold[54], maintaining the intrinsic properties of the polymer in the composite. Further, multi-walled CNT are suitable and economic for large scale applications[54]. The sensors have been integrated into a functionalized hand-glove able to monitor finger movements in real time, with applicability in areas such as health care, gaming and robotics devices. Thus, this the present work represents an important contribution in the optimization by scalable processing technologies and improved integration into devices of piezoresistive polymer-based materials for force and deformation sensor applications.

## 2. Materials and Methods

The material used as polymer matrix is a thermoplastic elastomer (TPE) triblock copolymer styrene-butadiene-styrene (SBS), composed by 80% of polybutadiene and 20% of polystyrene with a radial block structure (C401 from Dynasol Elastomers). This TPE is characterized by stretchability and easy recovery, presenting low mechanical hysteresis[55]. To increase the electrical conductivity of the insulating matrix, multi-walled carbon nanotubes (CNT) with reference NC7000 from Nanocyl were used. The

CNT show an average diameter of 9.5 nm, length of 1.5 μm, 90% of purity and surface area of the 250-300 $m^2/g$. For the preparation of the printed sensors toluene (purity ≥99.9%, density 0.87 $g/cm^3$; Sigma-Aldrich) was used as solvent. Figure 1 summarizes the materials and processes used in the present work.

### *2.1 Composites preparation*

Polymer composites were prepared by extrusion and spray printing techniques, in order to evaluate processability, scalability of the production and potential implementation of these materials into device applications. Multifunctional materials can be tailored using different processing methods to allow improved integration into devices.

#### *2.1.1 Extrusion*

Extrusion processing was carried out with a co-rotating mini-extruder Microlab Twinscrew from Rondol Technology Ltd, with a screw diameter of 10 mm and a length of 200 mm and a circular die of 1 mm, which means that the diameter of the composite, after extrusion, is near 1.5 mm.

The processing conditions, screw rotation velocity and temperature were optimized for the CNT/SBS composites at 35 rpm rotational speed and the temperature (5 zones from feed to die zone, increasing from 150 to 190 ºC) profile along the extruder as shown in Figure 1.

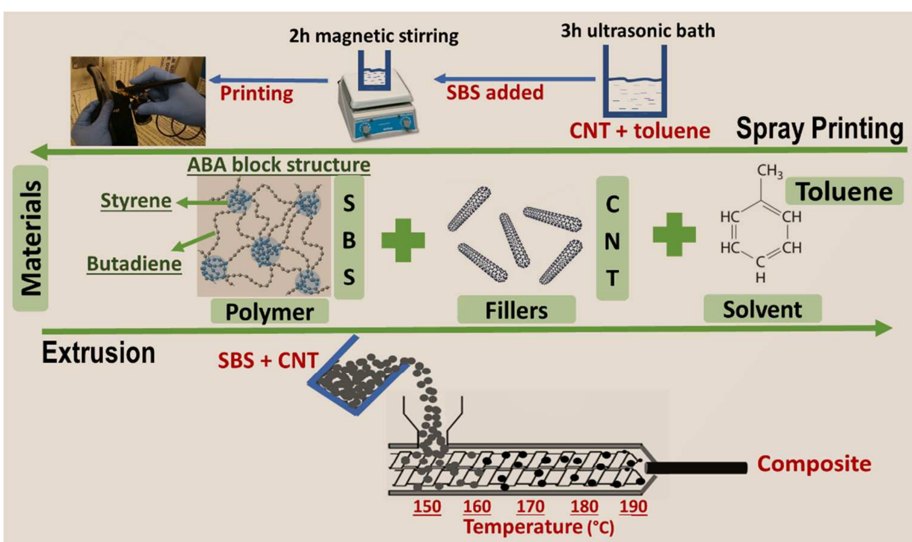


Figure 1- Materials and methods used for the preparation of the piezoresistive composites. Above: spray printing procedure; middle: materials; below: extrusion procedure.

The CNT contents used for the preparation of the composites was 0, 4, 6, 8 and 10 weight percentage (wt.%). Before the extrusion, the SBS and the CNT were manually mixed and shacked in a glass bottle. After extrusion, the composites were cooled to room temperature. Further experimental description is detailed in[34].

#### *2.1.2 Spray printing*

Tailoring the rheological properties of the piezoresistive inks allows their suitable integration into specific devices as well as the implementation of the sensors by additive manufacturing methods[53, 56]. Spray printing or drop casting are appropriated methods to develop printed films, spray printing being easily implemented on a larger scale[56].

The inks for spray printing of the composites were prepared by using 1 g of SBS for 6 ml of toluene with a viscosity of the piezoresistive inks between 744 and 1490 cP, evaluated with a Physica MCR 300 Modular Compact Rheometer at shear rates between 0 and 1600 $s^{-1}$. The ink was prepared as follow: the amount of CNT (1 and 2 wt.%, as it has been shown to have excellent piezoresistive properties[49]) was placed in an Erlenmeyer with the corresponding amount of toluene, and placed in an ultrasonic bath (Sonorex Super – RK 106) for approximately 3 h, to obtain disagglomeration and good CNT dispersion. After this step, SBS was added to the solution and placed on a magnetic stirrer until complete dissolution of the polymer. Toluene is used to dissolve the SBS and to obtain a good dispersion of CNT, which leads to a decrease of the electrical percolation threshold, compared to extruded composites[34]. After ink preparation, the material was printed with an air gun pistol (Clarke Diy Air Brush-CAB1H) at a pressure of 3 bar. The sensors were then placed in an oven (Binder E, model 28) at a temperature of 60 ºC during 1 h for total solvent evaporation. The final thickness of the sensor was around 40 µm. More details on the processing of piezoresistive inks can be found elsewhere.

### *2.3 Materials and sensor characterization*

#### *2.3.1 Mechanical measurements*

Mechanical measurements in extruded wires composites were performed with a universal testing machine, Shimadzu AG-IS, with a 50 N load cell in uniaxial stress mode. Tests were performed at room temperature until rupture for each sample at a velocity of 5 mm/min. Three measurements were performed for each sample. The initial modulus was calculated up to 5% of strain for all samples. The mechanical hysteresis of the materials was characterized after ten stress-strain cycles, for several deformations from 5, 10, 20 to 50% at a velocity of 5 mm/min.

### *2.3.2 Electrical measurements*

The electrical resistivity ($\rho$) of the both composites was calculated from the slope of the curves I-V, measured with a 6487 Keithley Picoammeter/Voltage Source. The electrical conductivity ($\sigma$) corresponds to the inverse of the electrical resistivity. The I-V data were measured at the surface of the extruded wires and spray printed composites samples with conductive silver ink deposited as electrodes at ≈15 mm of distance between them. Measurements were obtained with the applied voltage ranging from -1 to +1 V, in steps of 0.1 V.

### *2.3.3 Piezoresistive measurements*

The piezoresistive tests were performed by measuring in real time the mechanical and electrical response of the composites. The mechanical tests were performed in the Shimadzu AG-IS universal testing set-up by applying 10 load-unload cycles at different velocities and deformations while the electrical resistance was simultaneously recorded with an Agilent 34410A multimeter through silver electrodes (conductive silver ink from Agar, reference AGG3790) placed on the composites.

Different measurement configurations were used for the extruded and printed composites, as represented in Figure 2: the 4-point-bending measurements (Figure 2A) for the printed sensors and uniaxial stress (Figure 2B) for the extruded wires.

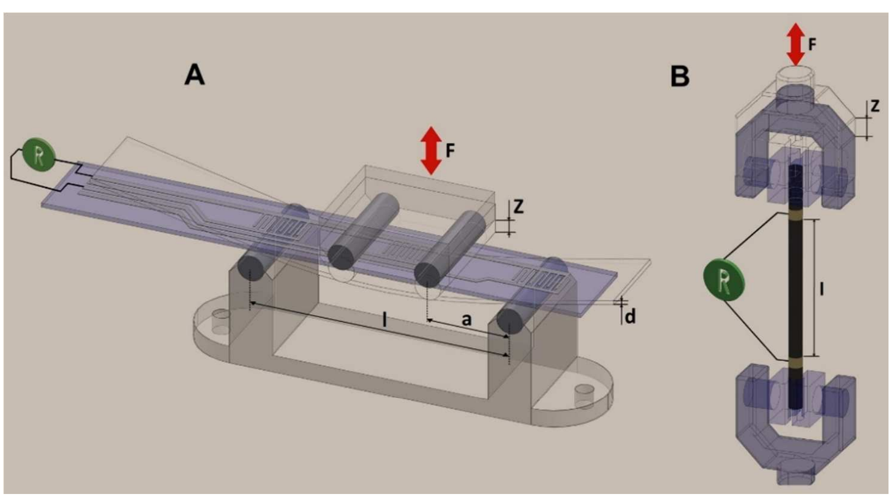

Figure 2- Piezoresistive measurements by *4-point-bending* tests (A) for the spray printed composites, where the distance between first and second bending point is $a$=15 mm, $z$ is the transversal deformation applied to the sample, $d$ is the thickness of the sample (near 1 mm) and the distance between both lower bending points $l$=50 mm. Piezoresistive measurements by uniaxial stretching (B) for the extruded composites, with 1.5 mm of diameter and 20 mm of distance. The silver electrodes are placed within the claws for better electrical contact.

The variation of the electrical resistance under mechanical solicitation and the corresponding piezoresistive sensibility were calculated for each loading-unloading cycle and provided as the value of the piezoresistive sensibility. For the uniaxial stress piezoresistive tests, 10 load-unload cycles were performed up to 20% of deformation at a test velocity from 1 to 50 mm/min. For the *4-point-bending* tests 5 load-unload cycles were performed up to 4 mm of displacement at a test velocity of 10 mm/min. The sample strain in the *4-point-bending* measurements was calculated from the theory of pure bending of a plate to a cylindrical surface[49], using the equation 2.

$$\varepsilon = \frac{3dz}{5a^2} \quad (2)$$

where $z$ is the vertical displacement of the piston, $d$ is the sample thickness (near 1 mm) and $a$ is the distance between the two bending points (Figure 2A). The *GF* was calculated for each mechanical stress-strain cycle.

### *2.4 Development of patterned sensors by spray printing*

The development of the piezoresistive printed sensors started with the design of the interdigitated conducting electrodes pattern using silver ink and applied by screen printing (HPS-021LV, Novacentrix).

The sensors were prepared in two steps: first, the conductive silver ink patters were placed on the substrate by screen printing, and then the piezoresistive element (CNT/SBS composite with 2 wt.% filler content) was printed on top of the interdigitated electrodes by spray printing. Screen printing was carried out with a home-made set-up with a metallic base structure supporting the screen. The screen (from Sefar) has 62 monofilaments by cm with a tension of 17 N.

The conductive patterns (interdigitated formed by 11 conductive lines having 0.8 mm width and 0.8 mm between them) were printed by depositing the silver ink (HPS-021LV, Novacentrix) on the screen and subsequently spreading it with a squeegee over a polyethylene naphthalene (PEN) substrate (Teonex Q65HA, produced by Teijin DuPont Films) and on the hand glove. After the deposition over substrate, the conductive silver ink was cured for 1 h at 80 ºC in an oven Binder E, model 28.

### *2.5 Readout electronic circuit for the hand-glove application*

An optimized circuit for piezoresistive sensors was developed with high hardware efficiency and minimum power consumption[6]. The implemented architecture is based on open components (Figure 3A) and using a single readout circuit for all sensors, multiplexing the various sensors inputs to read all sensors sequentially. Being this an auto-adaptive circuit, the system changes automatically their hardware and firmware parameters according to the sensor to be measured, increasing accuracy without requiring a constant manual adjustment of the circuit.

Figure 3B illustration the schematic representation of the architecture of the adaptive readout circuit. The sensor is crossed by a constant current, generated using a digital current source (I), based on a voltage to current converter circuit, using the OPA2234, operational amplifier from Texas Instruments, and a digitally variable resistor AD5272 from Analog Devices, to modify the load current. When the sensor changes its resistance, it causes the voltage to change in the input of LTC6915 amplifier, G, which is a zero drift, precision instrumentation amplifier with digitally programmable gain, from Linear Technology, comparing this variation with the reference voltage (voltage when the sensor is at rest), generated in the digital-to-analogic converter circuit, AD8519 (DAC) from Analog Devices. This difference is amplified according to the digital gain defined by the firmware and the output voltage is converted to digital format by the analog-to-digital converter (ADC) circuit, present inside to microcontroller unity, μC, where the data is saved. For this circuit was selected SimpleLink™ Ultra-Low-Power Dual-Band Wireless microcontroller CC1350, from Texas Instruments. All circuit subparts are controlled by the μC using the serial peripheral interface, SPI, bus to communicate. The stored data are transmitted using a radio frequency, RF, channel to a remote platform that allows to evaluate the sensor variation according to the movement (Figure 3C).

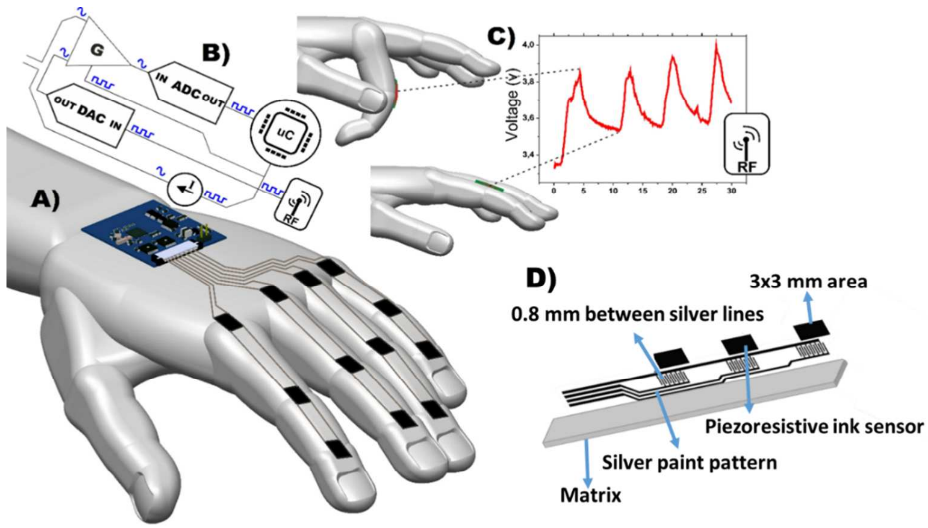


Figure 3- A) Implementation scheme of the sensors and readout circuit. B) Block diagram of the piezoresistive multi-sensor readout circuit. C) Example of the read circuit output sensor response. D) Schematic representation of the patterned sensor configuration for application in each finger characterization. The sensors are composed by a flexible polymer substrate PEN, and interdigitated electrical conducting patterns achieved through conductive ink and the piezoresistive material spray printed on top of the interdigitated patterns.

The interdigitated pattern (silver electrodes patter in Figure 3D for each sensor was designed with 11 interdigitated conductive lines of 5×0.8 mm of length and width, respectively, with 0.8 mm distance between silver lines to the lecture of the sensors sensibility. As the sensors are to be implemented in a hand-glove, three sensors were printed in a row (Figure 3D) for each finger, one for each finger joint to evaluate their motion behaviour. On top of each interdigitated conducting geometry the piezoresistive ink was deposited with an area of 3×3 cm. Thus, whenever the fingers movement, the variations of the electrical resistance of each sensor is measured.

For this application the system operates at a rate of 20 Hz, which corresponds to a reading rate of 240 Hz per each sensor.

## 3. Results and Discussion

The obtained results and the corresponding discussion are presented in this section to highlight the differences between the composites obtained by the different preparation methods in terms of mechanical, electrical and piezoresistive response.

### *3.1 Electrical and mechanical properties of the composites*

The electrical conductivity measurements for the different composite samples obtained by the two processing methods (extruded and spray printed) are shown in Figure 4.

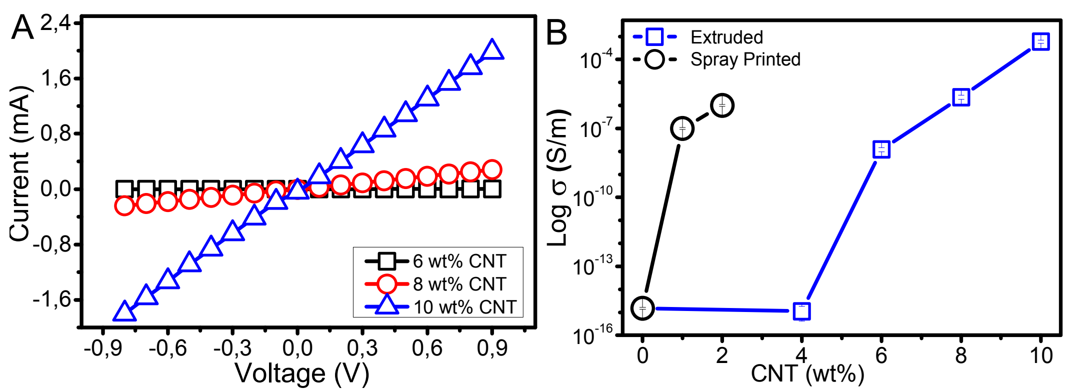


Figure 4- A) Representative current-voltage curves for the CNT/SBS extruded composites with 6, 8 e 10 wt.% CNT content. B) Electrical conductivity for the extruded (□) and spray printed (○) composites as a function of filler content.

Figure 4 shows that the electrical conductivity of the composites increases with increasing filler content, as indicated by the increasing slope of the I-V characteristic curves (Figure 4A). The remaining I-V curves present similar behaviour, for their respective electrical conductivity, with those shown in Figure 4A. The increase of the electrical conductivity and the presence of a percolation threshold occurs both for extruded and spray printed composites, being the percolation threshold at lower concentrations for the latter, which is attributed to a better CNT dispersion[34] as well as the alignment of the nanofillers in the extruded composites that increases for low fibre diameter and with higher shear rates within the process, leading to increased percolation threshold[57]. Thus, for extruded composites up to 4 wt.% CNT contents, the composites show an electrical conductivity similar to SBS, and for CNT contents above 4 wt.% a strong increase of the electrical conductivity is observed, being the percolation threshold near to 6 wt.% of CNT content. The electrical conductivity of the composites with 10 wt.% CNT is near $6\times10^{-4}$ S/m. For spray printed composites a similar behaviour is observed, but with the percolation threshold at filler concentrations near to 1 wt.%. Processing method and filler dispersion have strong influences in the electrical properties of the CNT/SBS composites. The percolation threshold and maximum conductivity of the composites agrees with the literature related to carbonaceous/elastomer composites[4].

The stress-strain characteristic curves of the samples prepared by extrusion are shown in Figure 5A. The spray printed composites prepared by solvent casting show similar mechanical characteristics, as also observed in[55, 58]. Figure 5A shows a maximum strain at break between 800 and 1100% and an increment of the maximum sustained stress level upon CNT content. Figure 5B shows that the initial modulus increases with increasing CNT content in the composites up to filler contents of 10 wt.% of CNT. Spray printed composites show maximum strain near 1000%[55], similar to extruded materials.

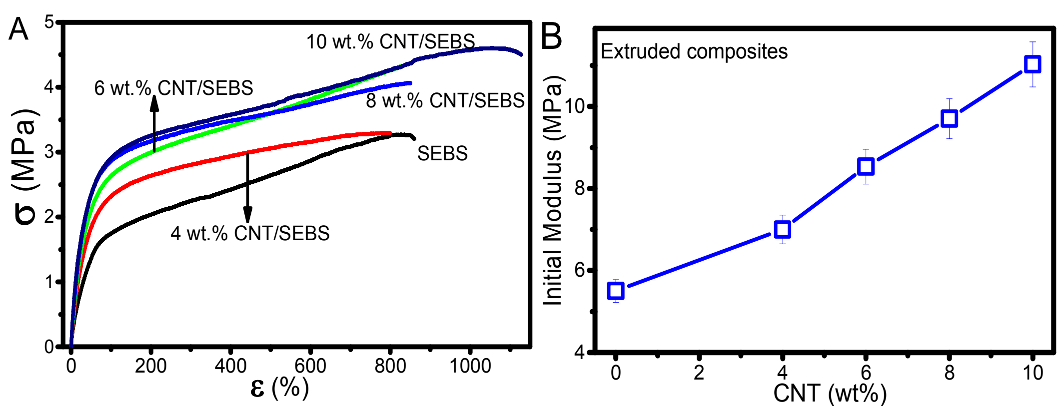


Figure 5- A) Stress-strain characteristic curves until rupture for the extruded CNT/SBS composites for several filler concentrations at a test velocity of 5 mm/min. B) Initial modulus of extruded pristine SBS and CNT/SBS composites, measure until 5% of strain.

The extruded composites show excellent mechanical properties for the development of large strain piezoresistive sensors with a large elastic region, where the yield strain is between 20% and 40% of strain, decreasing with increasing CNT content in the composites (Figure 5A). The maximum stress increases with increasing CNT content in the composites being lower than 5 MPa for the CNT/SBS composites with 10 wt.% CNT, as can be observed in Figure 5A. Further, the initial modulus of the CNT/SBS extruded composites (Figure 5B) also increases linearly with increasing CNT content. The relative increase upon the initial modulus, when comparing SBS with the composite with 10 wt.% CNT, is around 100%, from around 5.5 to 11 MPa. Extruded composites present excellent electrical properties (both overall electrical conductivity and electrical percolation threshold) and mechanical properties, with yield strain around 50% and large maximum strain.

Spray printed composites (data not shown) show similar maximum strain (≈1000%) than extruded samples, but lower yield strain[55]. The initial modulus also increases with increasing CNT content in the composites, with values ranging from 1.4 to 3.2 MPa for SBS and CNT/SBS with 2 wt.% CNT content, respectively.

As both processing method shows similar mechanical properties, but extruded materials typically show more oriented microstructure polymer chains, leading to higher initial modulus than spray printed composites, with randomly oriented microstructural features. Extruded composites will be analysed in detail, being the results, nevertheless similar for both composites, considering the differences in the initial modulus. The elastomeric characteristics of the composites are reduced with respect to pristine SBS (Figure 5A), which can be also observed in the dissipated energy of the stress-strain cycles (Figure 6, for extruded composites) for different deformations and test velocities. The mechanical hysteresis of SBS in 10 stress-strain cycles at strains from 5% to 50% and at a test velocity of 5 mm/min, is shown in Figure 6B.

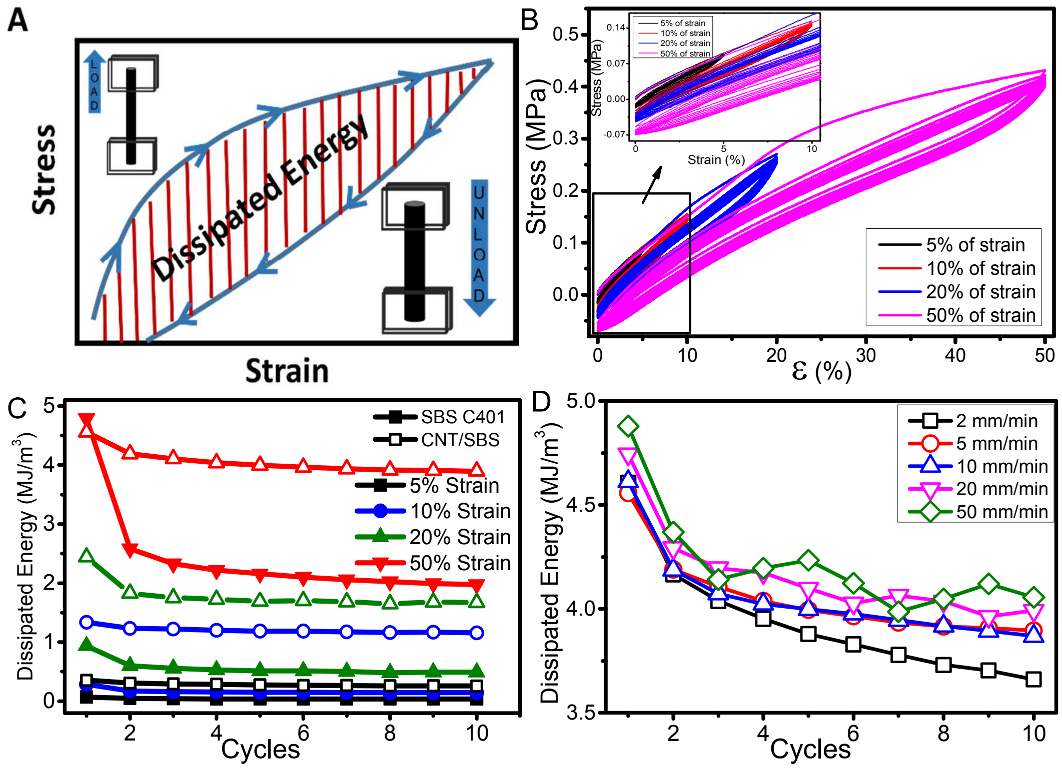


Figure 6- A) Illustration of typical stress-strain tests and dissipated energy evaluation in each load-unload cycle. B) Hysteresis corresponding to 10 mechanical stress-strain cycles for SBS, at 5, 10, 20 and 50% maximum deformation at a deformation speed of 5 mm/min. C) Dissipated energy for SBS and CNT/SBS composites with 8 wt.% CNT for different maximum deformations at testing velocity of 5, 10, 20 and 50 mm/min, for 10 cycles. D) Dissipated energy for CNT/SBS composites with 8 wt.% CNT at different testing velocities of 2, 5, 10, 20 and 50 mm/min for a strain of 50%.

The suitable characterization of the mechanical hysteresis (stretching and elastic recovery) is critical for the proper evaluation of the reproducibility and reliability of the sensors. The mechanical hysteresis increases with increasing strain and is larger for the initial cycles, as shown in Figure 6C. The dissipated energy can be obtained through the area of each stress-strain cycle[34] and increases with the applied strain on the composites when compared to SBS (Figure 6C). Therefore, also increases the initial modulus, Figure 5B, of the composites  for larger fillers contents due to the better stress transfer between the polymer matrix and the CNT[59]. Thus, the CNT not only increase the electrical conductivity, but also reinforces the mechanical properties of the composites. As this reinforcement is proportional to the inverse of the CNT diameter, it is suggested that initial modulus scales directly with the total interfacial surface in the composites[59]. The composites with CNT show a higher energy loss under each cyclic deformation, compared to pure SBS (Figure 6C). Although the hysteresis increases with strain, both the pristine polymer and the corresponding composites show easy recover after larger deformations.

To analyses the influence of the test velocity on the dissipated energy (Figure 6D), the mechanical tests performed at velocities between 2 and 50 mm/min in the extruded CNT/SBS composite with 8 wt.% fillers contents show that the dissipated energy increases with increasing test velocity and decreases with increasing number of cycles for each velocity, in particular for the initial cycles. This phenomenon can be attributed to initial modulus and consequent stress-induced stiffening at larges strains were both found to increase with increasing filler content[60].

Thus, both extruded and spray printed composites show interesting mechanical and electrical properties to work as sensors from low to larger deformations. The processing method influences the electrical and mechanical properties of the composites, allowing to tailor their properties for specific applications and allowing simple integration into devices. Extruded composites show a larger percolation threshold concentration, leasing also to mechanical properties with large maximum strain and low hysteresis.

### *3.2 Piezoresistive response*

The piezoresistive response was evaluated under uniaxial strain for extruded composites and in *4-point-bending* experiments for spray printed composites sensors. The composites selected or the evaluation of the piezoresistive response are the ones with 8 wt.% CNT content for the extruded composites and the ones with 1 wt.% CNT content for the spray printed composites. This materials selection has been performed as it has been demonstrated that for large deformation of the composites, the CNT content must be close to but above the percolation threshold in order maximize the piezoresistive response and not to lose electrical percolation during the stretching process[61], until larger strains.

The piezoresistive properties of this type of composites is attributed to a tunnelling effect mechanism[54, 62]. The tunnel resistance depends on the materials within the composite (polymer and reinforcement filler) and the maximum tunnelling distance can vary from 2 to 5 nm[54]. The intrinsic conductivity and aspect ratio of the nanofillers is one essential factor which governs the percolation threshold and the piezoresistive behaviour of the composites[54].

During loading-unloading mechanical cycles the electrical resistance will change due to geometrical factors and to variations of the conductive network. Piezoresistive sensibility thus will depend on extrinsic and intrinsic contributions (Eq. 1), where the extrinsic contribution depends on the Poisson coefficient. *GF* values larger than the extrinsic contribution depend on modifications of the conductive network and therefore by the tunnelling effect. The mechanisms which govern the changes in conductive network during mechanical stimulus are: reconstruction of the conductive network (variations on conductive pathways), changes in the contact resistance between fillers, and changes in the filler-to-filler interparticle distance[54, 62]. These processes coexist in the composite during the loading and unloading cycles, with composites showing similar behaviour for all cycles (Figure 7A). The piezoresistive sensibility near the electrical percolation threshold shows the highest values, mainly due to the effect of the variations in the tunnelling distance with applied strain, which plays an essential role in determining the piezoresistive response[13]. The loading-unloading measurements indicate that the sensors with higher filler content show better stability with lower sensibility, which is attributed to a more robust conductive network, due to the larger filler content, which is therefore less sensitive to strain induced variations[62].

### *3.2.1 Extruded composites*

The piezoresistive response was obtained by measuring the variation of the electrical resistance under the application of a uniaxial mechanical deformation during several stress-strain cycles (Figure 7). The *GF* was calculated after linear fitting with equation 1. Figure 7A shows the experimental measurements to illustrate the piezoresistive response (ε versus $\Delta R/R_0$ with time) for 10 loading-unloading cycles under uniaxial stretching for the extruded CNT/SBS composites with 8 wt.% CNT content and Figure 7B the *GF* as a function of maximum strain at a test velocity of 10 mm/min.

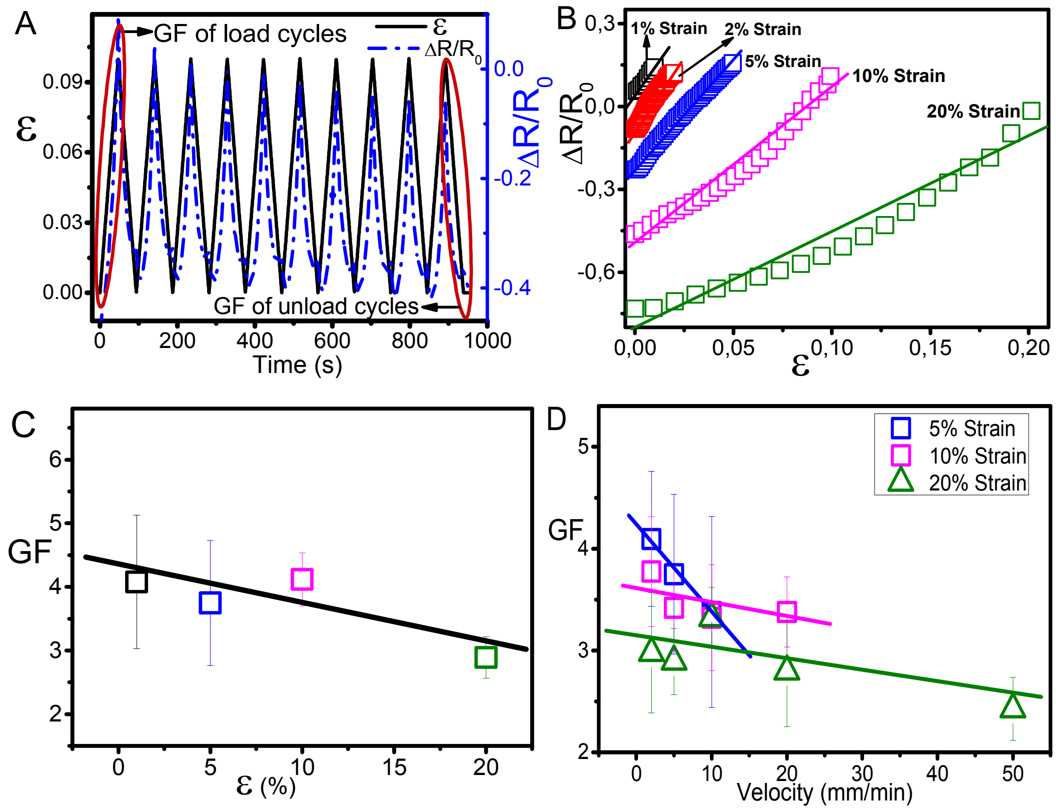


Figure 7- Piezoresistive measurements under uniaxial strain for the extruded CNT/SBS composites with 8 wt.% CNT content. A) Piezoresistive measurements for 10 loading-unloading cycles for 1% of maximum strain, B) Linear fit for *GF* calculus up to 20% of strain. The piezoresistive sensibility is presented in function of strain (at 5 mm/min) C) and velocity with several strains D).

The extruded CNT/SBS composite with 8 wt.% CNT shows excellent piezoresistive properties with electrical resistance variations following linearly the external mechanical loading-unloading cycles (Figure 7A) from small to large applied strain. The CNT/SBS composite behaviour and the respective piezoresistive sensibility is shown in Figure 7B from low strain up to 20% of strain. The slope of the linear fit between the strain and the electrical resistance decreases with increment upon the strain in the composite. Piezoresistive sensibility in function of the applied strain (up to 20%) is between $3 < GF < 4$, decreasing slightly for larger applied strain in composite, at 5 mm/min (Figure 7C). Up to 10% of strain, the piezoresistive sensibility is similar. Comparing the *GF* of the extruded composites for several velocities for the same deformation it is possible conclude that piezoresistivity decreases with the increase of the velocity for 5% of strain, from $GF \approx 4.4$ to $GF \approx 3.4$, between 1 to 10 mm/min. To the larger strains (10 and 20%) the piezoresistivity is practically constant in function of the velocity, with slightly decrease for measures in 20% of strain, with increase of the velocity. The piezoresistive sensibility is higher in the percolation threshold zone, but the linearity for composites until larger strain decreases for composites near percolation threshold[49]. Previous studies have shown that the CNT/SBS-family of piezoresistive composites support large number of cycles with large stability, even at large strains, the relative resistance variation stabilizing after few tens of cycles[5-6]. Further, the composites practically have no degradation, suggesting that CNT works as a photostabilizer in the composites[39]. Thus, the extruded materials show excellent mechanical and electrical properties to be used as piezoresistive large strain sensors, with piezoresistive response and physico-chemical stability for long-cycles utilization.

### *3.2.2 Spray printed sensors*

The typical behaviour of the *4-point-bending* test for the spray printed sensors are presented in Figure 8. Five stress-strain cycles of the spray printed composite with 1 wt.% CNT are presented for deformations up to 4 mm of strain and a test velocity of 10 mm/min for different loading-unloading cycles. Besides the extruded composites, the spray printed materials also have piezoresistive properties, showing the wide range of applicability using this kind of materials.

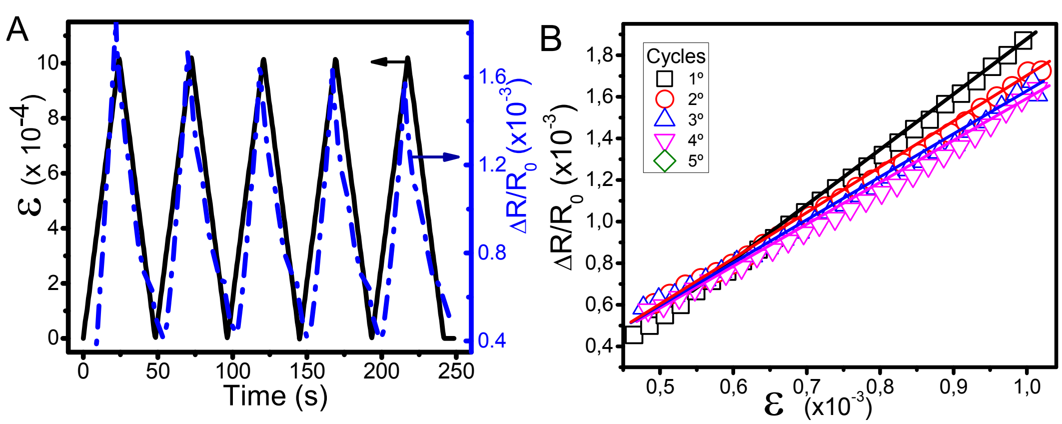


Figure 8- Piezoresistive measurement behaviour for the spray printed composite with 1 wt.% CNT content under *4-point-bending* measurements A) measure at 4% strain and 10 mm/min. B) Piezoresistive sensibility (*GF* calculus) for the cycles number for 4% strain at 10 mm/min.

The piezoresistive response was analysed for material prepared by spray printed method. The composite 1 wt.% CNT content were measure for strains from 1 and 4 mm. Spray printed sensors show *GF* values between 1 and 1.5 independently of the strain (up to 4 mm) or even for several velocities (between 1 to 10 mm/min). Spray printed composites with 2 wt.% CNT also shows similar behaviour than composite with 1 wt.%. In this way, *4-point-bending* method influences the *GF* of the composites. Presenting lower strain (the distance variation between silver electrodes is smaller) the *GF* is lower than composites measure by uniaxial stress, as reported in literature[58].

Comparing the results of extruded composites and printed sensors, higher values of *GF* were obtained for the extruded composites as they were subjected to higher deformations, and different measurement method. However, both can be used as piezoresistive sensors, from low to larger deformations, with excellent linearity between electrical and mechanical properties.

The mechanical properties of both processed materials are similar with larger yielding for extruded composites due to the oriented microstructural features, typical of this processing method. Further, the initial modulus of the composites increases with increasing CNT content in both composites. Spray printing shows better CNT dispersion and lower percolation threshold compared to extruded composites. Mechanical hysteresis increases with increasing CNT in the composite and with applied strain, decreasing with the number of cycles, up to 10 cycles. The deformation speed has no influence in the hysteresis, for the evaluated conditions.

Piezoresistive response was evaluated taking into account the final application. Thus, uniaxial strain was applied to the extruded material and *4-point-bending* tests for the spray printed composites, both in order to evaluate the movement of the fingers in a piezoresistive glove (Figure 9).

The uniaxial stress for extruded composites and *4-point-bending* for spray printing composites are carried out based in the glove application geometry of the electrodes. The *4-point-bending* piezoresistive measurements is more appropriate due to the configuration of the silver ink deposited in the glove. Uniaxial stress is more appropriate for extruded composites because de composite is stretched during the finger movement.

Both methods show good piezoresistive response, but extrusion can be considered environmentally-friendlier than spray printing, considering that no solvent is used. Porous structures (as textile mesh) need several layers of ink to present homogeneous behaviour. Both composites, obtained after the different processing methods, show good overall properties to be used in application, the bandwidth of the piezoresistive sensors being determined by the mechanical relaxation of the matrix[1].

### *3.3 Piezoresistive sensors application*

A hand glove was used as a *proof-of-concept* of the applicability of these piezoresistive composites as sensors. These tests were performed in both extruded and spray printed sensors (Figure 9) and the wireless electronic circuit was used to read, in real time, the sensors response and to save it to the computer (Figure 9B). Conductive silver ink was screen printed over the glove finger to serve as conductive electrodes of the spray-printed sensors (Figure 9A). The extruded wires, on the other hand, were sewed to the hand glove (Figure 9B) and the electrodes were placed at the tips of the wires. Both application methods present good piezoresistive response, with similar electromechanical sensibility in the previously presented tests. On the other hand, the extrusion method shows some advantages in the sense that no interdigitates are required for signal acquisition and that can be considered environmentally friendlier than spray printing, as it does not use solvents during the preparation of the composites. On the other hand, spray printing has the advantage of being very flexible in the types of material and geometries in which the sensors can be integrated to. It is also a very fast and low-cost processing method.

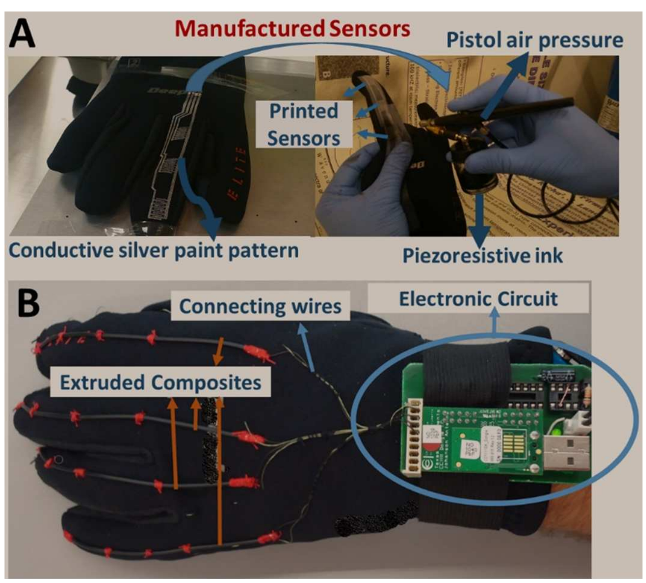

Figure 9- Piezoresistive sensors applied by spray printing (A) and extruded wires sewed to the hand-glove (B).

The piezoresistive response of the glove hand sensors is shown in Figure 10 for finger movement at the same time and for the movement of the individual fingers. Sensor 1 to 4 represent the different fingers (excluding the thumb).

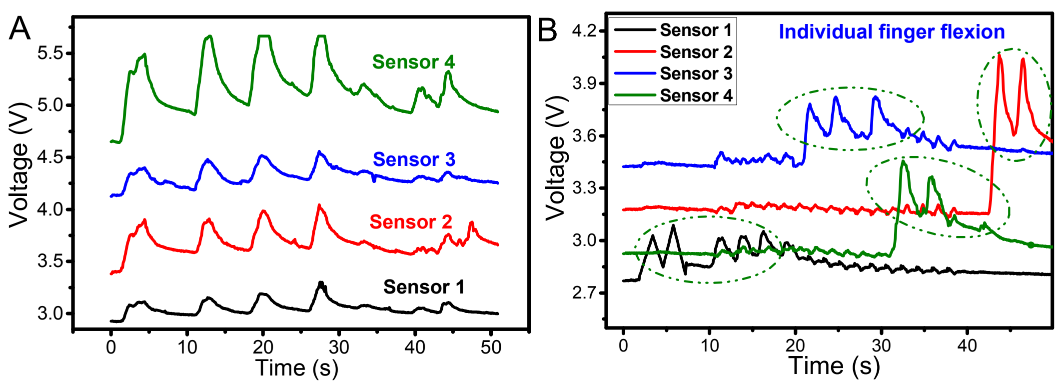


Figure 10- Voltage output of the 4 sensors- one for each finger, excluding the thumb- for the extruded composites when all fingers are simultaneously (a) or individually (b) deflected. See supporting video.

Figure 10 shows that the variation of the electrical voltage of the composites increases when the finger is deflected and the piezoresistive sensors stretched. The electrical response is proportional to the strain and recovers the initial values when the finger returns to the original position. The extruded composite shows similar piezoresistive behaviour than spray printed composite. On the other hand, extruded composites work until larger deformations, once the silver ink can break and interrupt the electrical connection on the spray printed glove device.

Thus, the present work fully demonstrates the applicability of extruded and spray printed piezoresistive SBS based composites sensors for strain sensing applications, opening the way for application in areas such as robotics, health care, structural health monitoring and entertainment, among other.

## 4. Conclusions

It has been shown that piezoresistive sensors can be developed for large strain sensing applications using a SBS thermoplastic elastomer polymer matrix reinforced with carbon nanofillers as conductive material. Further, these sensors can be prepared by extrusion or spray printing techniques that allow scaling-up and integration into devices, as well tailoring the sensors for specificity of the application. Large maximum strain (> 800%) and yield strains (between 20 to 40%) and the percolation threshold near 1 and 6 wt.% of CNT for spray printed and extruder composites, respectively, make these composites ideal polymer-based sensors to strain applications. Larger strain and easy recovery with lower mechanical hysteresis characterizes these piezoresistive sensors. The excellent linearity between the strain and electrical resistivity variations allows these materials to be applied as piezoresistive sensors, with piezoresistive sensibility around $GF \approx$ 3 to 4 for extruded and $GF \approx$ 1 to 1.5 for spray printed composites. Processing method and filler content influences the piezoresistive sensibility of the materials, allowing to tailor materials response for specific applications.

The developed materials were integrated, together with the readout and wireless communication system, into a hand glove and it was demonstrated their suitability for the monitoring of finger movements. Thus, the optimization and up-scalable processability of polymer based piezoresistive materials based on SBS and CNT has been demonstrated, together with their suitable integration as deformation sensor in a proof of concept application. In this way, a solution is presented that can be implemented in a large range of applications, where force and deformation sensing is required.

**Acknowledgments**

This work was supported by the Portuguese Foundation for Science and Technology (FCT) in the framework of the Strategic Funding UID/FIS/04650/2013, project PTDC/EEI-SII/5582/2014 and grants SFRH/BPD/110914/2015 and SFRH/BPD/97739/2013 (PC and VC, respectively). The authors acknowledge funding by the Spanish Ministry of Economy and Competitiveness (MINECO) through the project MAT2016-76039-C4-3-R (AEI/FEDER, UE) and from the Basque Government Industry Department under the ELKARTEK and HAZITEK program.

**Supporting Information Available:** A video of a hand glove prototype is presented with the extruded wires as sensors for the moving fingers. The electronic circuit with wireless communication to a computer is also shown.

# References

1. Deng, H.; Lin, L.; Ji, M. Z.; Zhang, S. M.; Yang, M. B.; Fu, Q., Progress on the Morphological Control of Conductive Network in Conductive Polymer Composites and the use as Electroactive Multifunctional Materials. *Prog Polym Sci* **2014,** *39* (4), 627-655.

2. Yang, T. T.; Xie, D.; Li, Z. H.; Zhu, H. W., Recent Advances in Wearable Tactile Sensors: Materials, Sensing Mechanisms, and Device Performance. *Mat Sci Eng R* **2017,** *115* (Supplement C), 1-37.

3. Ponmozhi, J.; Frias, C.; Marques, T.; Frazao, O., Smart Sensors/Actuators for Biomedical Applications: Review. *Measurement* **2012,** *45* (7), 1675-1688.

4. Sadasivuni, K. K.; Ponnamma, D.; Thomas, S.; Grohens, Y., Evolution from Graphite to Graphene Elastomer Composites. *Prog Polym Sci* **2014,** *39* (4), 749-780.

5. Gonçalves, B. F.; Oliveira, J.; Costa, P.; Correia, V.; Martins, P.; Botelho, G.; Lanceros-Mendez, S., Development of Water-Based Printable Piezoresistive Sensors for Large Strain Applications. *Composites Part B: Engineering* **2017,** *112* (Supplement C), 344-352.

6. Gonçalves, B. F.; Costa, P.; Oliveira, J.; Ribeiro, S.; Correia, V.; Botelho, G.; Lanceros-Mendez, S., Green Solvent Approach for Printable Large Deformation Thermoplastic Elastomer Based Piezoresistive Sensors and their Suitability for Biomedical Applications. *Journal of Polymer Science Part B: Polymer Physics* **2016,** *54* (20), 2092-2103.

7. Zhao, H.; Bai, J., Highly Sensitive Piezo-Resistive Graphite Nanoplatelet-Carbon Nanotube Hybrids/Polydimethylsilicone Composites with Improved Conductive Network Construction. *ACS Appl Mater Interfaces* **2015,** *7* (18), 9652-9.

8. Wei, Y.; Torah, R.; Li, Y.; Tudor, J., Dispenser Printed Capacitive Proximity Sensor on Fabric for Applications in the Creative Industries. *Sensor Actuat A-Phys* **2016,** *247* (Supplement C), 239-246.

9. Savage, M. J., Field Evaluation of Polymer Capacitive Humidity Sensors for Bowen Ratio Energy Balance Flux Measurements. *Sensors* **2010,** *10* (8), 7748-71.

10. Jeong, B.; Gutowska, A., Lessons From Nature: Stimuli-Responsive Polymers and their Biomedical Applications. *Trends in Biotechnology* **2002,** *20* (7), 305-311.

11. Huang, J.; Wang, J.; Yang, Z.; Yang, S., High-Performance Graphene Sponges Reinforced with Polyimide for Room-Temperature Piezoresistive Sensing. *ACS Appl Mater Interfaces* **2018,** *10* (9), 8180-8189.

12. Tiwana, M. I.; Redmond, S. J.; Lovell, N. H., A Review of Tactile Sensing Technologies with Applications in Biomedical Engineering. *Sensor Actuat A-Phys* **2012,** *179* (Supplement C), 17-31.

13. Vertuccio, L.; Guadagno, L.; Spinelli, G.; Lamberti, P.; Tucci, V.; Russo, S., Piezoresistive Properties of Resin Reinforced with Carbon Nanotubes for Health-Monitoring of Aircraft Primary Structures. *Compos Part B-Eng* **2016,** *107* (Supplement C), 192-202.

14. Stassi, S.; Cauda, V.; Canavese, G.; Pirri, C. F., Flexible Tactile Sensing Based on Piezoresistive Composites: A Review. *Sensors* **2014,** *14* (3), 5296-332.

15. Freynik, H. S., Jr.; Roach, D. R.; Deis, D. W.; Hirzel, D. G., Evaluation of Metal-Foil Strain Gauges for Cryogenic Application in Magnetic Fields. In *Advances in Cryogenic Engineering*, Timmerhaus, K. D.; Reed, R. P.; Clark, A. F., Eds. Springer US: 1978; Vol. 24, Pp 473-479.

16. Knechtel, R., Single Crystalline Silicon Based Surface Micromachining for High Precision Inertial Sensors: Technology and Design for Reliability. *Microsyst Technol* **2010,** *16* (5), 885-893.

17. Gonçalves, V.; Brandão, L.; Mendes, A., Development of Porous Polymer Pressure Sensors Incorporating Graphene Platelets. *Polymer Testing* **2014,** *37* (0), 129-137.

18. Falletta, E.; Costa, P.; Della Pina, C.; Lanceros-Mendez, S., Development of High Sensitive Polyaniline Based Piezoresistive Films by Conventional and Green Chemistry Approaches. *Sensor Actuat A-Phys* **2014,** *220* (0), 13-21.

19. Han, J. E.; Kim, D.; Yun, K. S., All-Polymer Hair Structure with Embedded Three-Dimensional Piezoresistive Force Sensors. *Sensor Actuat A-Phys* **2012,** *188* (0), 89-94.
20. Aryafar, M.; Hamedi, M.; Ganjeh, M. M., A Novel Temperature Compensated Piezoresistive Pressure Sensor. *Measurement* **2015,** *63* (0), 25-29.
21. Tung, T. T.; Yoo, J.; Alotaibi, F. K.; Nine, M. J.; Karunagaran, R.; Krebsz, M.; Nguyen, G. T.; Tran, D. N.; Feller, J. F.; Losic, D., Graphene Oxide-Assisted Liquid Phase Exfoliation of Graphite into Graphene for Highly Conductive Film and Electromechanical Sensors. *ACS Appl Mater Interfaces* **2016,** *8* (25), 16521-32.
22. Amarasinghe, R.; Dao, D. V.; Toriyama, T.; Sugiyama, S., Development of Miniaturized 6-Axis Accelerometer Utilizing Piezoresistive Sensing Elements. *Sensor Actuat A-Phys* **2007,** *134* (2), 310-320.
23. Gao, L. M.; Thostenson, E. T.; Zhang, Z.; Chou, T. W., Sensing of Damage Mechanisms in Fiber-Reinforced Composites under Cyclic Loading Using Carbon Nanotubes. *Adv Funct Mater* **2009,** *19* (1), 123-130.
24. Arboleda, L.; Ares, A.; Abad, M. J.; Ferreira, A.; Costa, P.; Lanceros-Mendez, S., Piezoresistive Response of Carbon Nanotubes-Polyamides Composites Processed By Extrusion. *J Polym Res* **2013,** *20* (12), 1-11.
25. Georgousis, G.; Pandis, C.; Chatzimanolis-Moustakas, C.; Kyritsis, A.; Kontou, E.; Pissis, P.; Krajci, J.; Chodak, I.; Tabciarova, J.; Micusik, M.; Omastova, M., Study of the Reinforcing Mechanism and Strain Sensing in a Carbon Black Filled Elastomer. *Compos Part B-Eng* **2015,** *80*, 20-26.
26. Georgousis, G.; Roumpos, K.; Kontou, E.; Kyritsis, A.; Pissis, P.; Koutsoumpis, S.; Micusik, M.; Omastova, M., Strain and Damage Monitoring in SBR Nanocomposites under Cyclic Loading. *Compos Part B-Eng* **2017,** *131*, 50-61.
27. Costa, P.; Nunes-Pereira, J.; Oliveira, J.; Silva, J.; Moreira, J. A.; Carabineiro, S. A. C.; Buijnsters, J. G.; Lanceros-Mendez, S., High-Performance Graphene-Based Carbon Nanofiller/Polymer Composites for Piezoresistive Sensor Applications. *Composites Science and Technology* **2017,** *153*, 241-252.
28. Tewari, A.; Gandla, S.; Bohm, S.; Mcneill, C. R.; Gupta, D., Highly Exfoliated MWNT-Rgo Ink-Wrapped Polyurethane Foam for Piezoresistive Pressure Sensor Applications. *ACS Appl Mater Interfaces* **2018,** *10* (6), 5185-5195.
29. Canavese, G.; Stassi, S.; Stralla, M.; Bignardi, C.; Pirri, C. F., Stretchable and Conformable Metal-Polymer Piezoresistive Hybrid System. *Sensor Actuat A-Phys* **2012,** *186* (0), 191-197.
30. Park, C. S.; Park, J.; Lee, D. W., A Piezoresistive Tactile Sensor Based on Carbon Fibers and Polymer Substrates. *Microelectron Eng* **2009,** *86* (4-6), 1250-1253.
31. Obitayo, W.; Liu, T., A Review: Carbon Nanotube-Based Piezoresistive Strain Sensors. *J Sensors* **2012,** *2012*.
32. Dubey, K. A.; Mondal, R. K.; Grover, V.; Bhardwaj, Y. K.; Tyagi, A. K., Development of a Novel Strain Sensor Based on Fluorocarbon-Elastomeric Nanocomposites: Effect of Network Density on the Electromechanical Properties. *Sensor Actuat A-Phys* **2015,** *221* (0), 33-40.
33. Avishek, R. A.; Chao, S.; Seong-Hyok, K.; Mark, G. A., An all-Polymer Airflow Sensor Using a Piezoresistive Composite Elastomer. *Smart Materials and Structures* **2009,** *18* (11), 115002.
34. Costa, P.; Silvia, C.; Viana, J. C.; Mendez, S. L., Extruded Thermoplastic Elastomers Styrene-Butadiene-Styrene/Carbon Nanotubes Composites for Strain Sensor Applications. *Compos Part B-Eng* **2014,** *57* (0), 242-249.
35. Wang, X.; Jiang, M.; Zhou, Z. W.; Gou, J. H.; Hui, D., 3D Printing of Polymer Matrix Composites: A Review and Prospective. *Compos Part B-Eng* **2017,** *110* (Supplement C), 442-458.

36. Robert, C.; Feller, J. F.; Castro, M., Sensing Skin for Strain Monitoring Made of PC-CNT Conductive Polymer Nanocomposite Sprayed Layer by Layer. *ACS Appl Mater Interfaces* **2012,** *4* (7), 3508-16.
37. Bonavolonta, C.; Camerlingo, C.; Carotenuto, G.; De Nicola, S.; Longo, A.; Meola, C.; Boccardi, S.; Palomba, M.; Pepe, G. P.; Valentino, M., Characterization of Piezoresistive Properties of Graphene-Supported Polymer Coating for Strain Sensor Applications. *Sensor Actuat A-Phys* **2016,** *252* (Supplement C), 26-34.
38. Zhao, X. H.; Ma, S. N.; Long, H.; Yuan, H.; Tang, C. Y.; Cheng, P. K.; Tsang, Y. H., Multifunctional Sensor based on Porous Carbon Derived from Metal-Organic Frameworks for Real Time Health Monitoring. *ACS Appl Mater Interfaces* **2018,** *10* (4), 3986-3993.
39. Costa, P.; Ribeiro, S.; Botelho, G.; Machado, A. V.; Mendez, S. L., Effect of Butadiene/Styrene Ratio, Block Structure and Carbon Nanotube Content on the Mechanical and Electrical Properties of Thermoplastic Elastomers after UV Ageing. *Polymer Testing* **2015,** *42* (Supplement C), 225-233.
40. Ribeiro, S.; Costa, P.; Ribeiro, C.; Sencadas, V.; Botelho, G.; Lanceros-Mendez, S., Electrospun Styrene-Butadiene-Styrene Elastomer Copolymers for Tissue Engineering Applications: Effect of Butadiene/Styrene Ratio, Block Structure, Hydrogenation and Carbon Nanotube Loading on Physical Properties and Cytotoxicity. *Compos Part B-Eng* **2014,** *67*, 30-38.
41. Zhao, S.; Li, J.; Cao, D.; Zhang, G.; Li, J.; Li, K.; Yang, Y.; Wang, W.; Jin, Y.; Sun, R.; Wong, C. P., Recent Advancements in Flexible and Stretchable Electrodes for Electromechanical Sensors: Strategies, Materials, and Features. *ACS Appl Mater Interfaces* **2017,** *9* (14), 12147-12164.
42. Li, Y.; Nie, M.; Wang, Q., Facile Fabrication of Electrically Conductive Low-Density Polyethylene/Carbon Fiber Tubes for Novel Smart Materials via Multiaxial Orientation. *ACS Appl Mater Interfaces* **2018,** *10* (1), 1005-1016.
43. Graillot, A.; Bouvet-Marchand, A.; Loubat, C., Specific Polymers - Functional Polymers and Materials for Optoelectronic Devices and Sensors. *Procedia Engineer* **2016,** *168* (Supplement C), 1581-1584.
44. Lu, Y., Industry 4.0: A Survey On Technologies, Applications and Open Research Issues. *Journal of Industrial Information Integration* **2017,** *6* (Supplement C), 1-10.
45. Jeong, T., Design and Modeling of Sensor Behavior for Improving Sensitivity and Performance. *Measurement* **2015,** *62* (0), 230-236.
46. Liao, Y. H.; Chou, J. C., Preparation and Characteristics of Ruthenium Dioxide for PH Array Sensors with Real-Time Measurement System. *Sensor Actuat B-Chem* **2008,** *128* (2), 603-612.
47. Dubuc, D.; Grenier, K., 16 - Radio Frequency (RF)-MEMS for Smart Communication Microsystems. In *Smart Sensors and Mems*, Nihtianov, S.; Luque, A., Eds. Woodhead Publishing: 2014; Pp 472-491.
48. Park, W.-T., Piezoresistivity. In *Encyclopedia of Nanotechnology*, Bhushan, B., Ed. Springer Netherlands: 2012; pp 2111-2117.
49. Costa, P.; Ferreira, A.; Sencadas, V.; Viana, J. C.; Lanceros-Mendez, S., Electro-Mechanical Properties of Triblock Copolymer Styrene-Butadiene-Styrene/Carbon Nanotube Composites for Large Deformation Sensor Applications. *Sensor Actuat A-Phys* **2013,** *201* (0), 458-467.
50. Nielsen, L. E., Morphology and the Elastic Modulus of Block Polymers and Polyblends. *Rheol Acta* **1974,** *13* (1), 86-92.
51. Bautista-Quijano, J. R.; Aviles, F.; Cauich-Rodriguez, J. V.; Schonfelder, R.; Bachmatiuk, A.; Gemming, T.; Rummeli, M. H., Tensile Piezoresistivity and Disruption of Percolation in Singlewall and Multiwall Carbon Nanotube/Polyurethane Composites. *Synthetic Metals* **2013,** *185*, 96-102.

52. Bautista-Quijano, J. R.; Aviles, F.; Cauich-Rodriguez, J. V., Sensing of Large Strain using Multiwall Carbon Nanotube/Segmented Polyurethane Composites. *J Appl Polym Sci* **2013,** *130* (1), 375-382.

53. Castro, H. F.; Correia, V.; Pereira, N.; Costab, P.; Oliveiraa, J.; Lanceros-Méndez, S., Printed Wheatstone Bridge With Embedded Polymer Based Piezoresistive Sensors for Strain Sensing Applications. *Additive Manufacturing* **2018,** *20*, 119-125.

54. Avilés, F.; Oliva-Avilés, A. I.; Cen-Puc, M., Piezoresistivity, Strain, and Damage Self-Sensing of Polymer Composites Filled with Carbon Nanostructures. *Advanced Engineering Materials* **2018,** *0* (0), 1701159.

55. Costa, P.; Silva, J.; Sencadas, V.; Simoes, R.; Viana, J. C.; Lanceros-Méndez, S., Mechanical, Electrical and Electro-Mechanical Properties of Thermoplastic Elastomer Styrene–Butadiene–Styrene/Multiwall Carbon Nanotubes Composites. *Journal of Materials Science* **2012,** *48* (3), 1172-1179.

56. Oliveira, J.; Correia, V.; Castro, H.; Martins, P.; Lanceros-Mendez, S., Polymer-Based Smart Materials by Printing Technologies: Improving Application and Integration. *Additive Manufacturing* **2018,** *21*, 269-283.

57. Qu, M.; Nilsson, F.; Schubert, D., Effect of Filler Orientation on the Electrical Conductivity of Carbon Fiber/PMMA Composites. *Fibers* **2018,** *6* (1), 3.

58. Costa, P.; Silva, J.; Anson-Casaos, A.; Martinez, M. T.; Abad, M. J.; Viana, J.; Lanceros-Mendez, S., Effect of Carbon Nanotube type and Functionalization on the Electrical, Thermal, Mechanical and Electromechanical Properties of Carbon Nanotube/Styrene-Butadiene-Styrene Composites for Large Strain Sensor Applications. *Compos Part B-Eng* **2014,** *61* (0), 136-146.

59. Coleman, J. N.; Khan, U.; Gun'ko, Y. K., Mechanical Reinforcement of Polymers using Carbon Nanotubes. *Adv Mater* **2006,** *18* (6), 689-706.

60. Cantournet, S.; Boyce, M. C.; Tsou, A. H., Micromechanics and Macromechanics of Carbon Nanotube-Enhanced Elastomers. *Journal of the Mechanics and Physics of Solids* **2007,** *55* (6), 1321-1339.

61. Teomete, E., Measurement of Crack Length Sensitivity and Strain Gage Factor of Carbon Fiber Reinforced Cement Matrix Composites. *Measurement* **2015,** *74*, 21-30.

62. Wang, X.; Meng, S.; Tebyetekerwa, M.; Li, Y.; Pionteck, J.; Sun, B.; Qin, Z.; Zhu, M., Highly Sensitive and Stretchable Piezoresistive Strain Sensor Based on Conductive Poly(Styrene-Butadiene-Styrene)/Few Layer Graphene Composite Fiber. *Composites Part A: Applied Science and Manufacturing* **2018,** *105*, 291-299.

## TOC